Tellus (2001), 53B, 205–219
Printed in UK. All rights reserved

TELLUS
ISSN 0280–6509

Measurements of atmospheric CO_2 from a meteorological tower in Tsukuba, Japan

By HISAYUKI YOSHIKAWA INOUE* and HIDEKAZU MATSUEDA, *Geochemical Research Department, Meteorological Research Institute, Nagamine 1-1, Tsukuba, Ibaraki 305-0052, Japan*

(Manuscript received 4 January 2000; in final form 16 January 2001)

ABSTRACT

Since February 1992, measurements of atmospheric CO_2 at 200 m above the ground have been taken from a meteorological tower (lat 36°04′ N, long 140°07′ E, 25 m a.s.l.) in Tsukuba, central Japan. A diurnal variation of atmospheric CO_2 at 200 m was clearly observed in summer and less clearly in winter. In summer, the maximum occurred a few hours after dawn and the minimum in the late afternoon; in winter, the CO_2 mixing ratio was fairly constant because of temperature inversion below 200 m. The daily mean values of atmospheric CO_2 in the afternoon (1300–1600 JST), selected as they were close to the representative values in the planetary boundary layer, were as high as 4 to 6 ppm greater than at stations in remote areas of the same latitudinal zone. This was mainly due to CO_2 emissions from anthropogenic sources in central Japan. The peak-to-trough amplitude of the seasonal variation, caused by the CO_2 exchange between the air and the land biosphere, ranged from 11 to 14 ppm. Year-to-year changes in the seasonal variation of atmospheric CO_2 during the period from May to July were correlated well with the surface air temperature among climate variables that affect the photosynthesis/respiration of the land biosphere. The change in CO_2 mixing ratio of the detrended seasonal variation from May to July increased with the surface air temperature, which was suggestive of the larger temperature dependence of respiration rate as compared with that of photosynthesis rate. Over the period from 1993 to 1999, the annual mean of the CO_2 mixing ratio increased from 363.0 ppm to 374.6 ppm. The growth rate from February 1992 to January 2000 showed a large interannual variability ranging from -0.8 to 4.6 ppm yr^{-1} with a mean rate of 2.0 ppm yr^{-1}.

1. Introduction

CO_2 is a greenhouse gas that has increased from about 280 ppm in pre-industrial times to 358 ppm in 1994 due to human activities (IPCC, 1995). Since the beginning of continuous measurements of atmospheric CO_2 in 1957/58 (Keeling et al., 1989), stations monitoring atmospheric CO_2 have been established at many sites throughout the world (Tans et al., 1998; WMO WDCGG, 2000). The objective of this global network is to investigate the global carbon cycle by using spatial and temporal variations in atmospheric CO_2 in combination with long-range transport models. However, as Tans (1991) has pointed out, current CO_2 monitoring sites are heavily weighted toward the marine boundary layer, and the CO_2 exchange between the air and the land biosphere is greatly under-represented. We need to provide CO_2 mixing ratios that are representative of regional/continental areas (Levin, 1987; Kuc, 1991; Levin et al., 1995; Bakwin et al., 1995, 1998; Haszpra, 1995; Schmidt et al., 1996; Yamamoto et al., 1999) to improve our knowledge of the CO_2 exchange between the air and the land on the basis of model simulations (Tans, 1991).

In February 1992, in order to examine the effect

* Corresponding author.
e-mail: hyoshika@mri-jma.go.jp

of CO_2 emissions due to fossil fuel combustion, and CO_2 exchange between the air and the land biosphere, we started measurements of atmospheric CO_2 at 200 m above the ground from a meteorological tower that stands in a field at the Meteorological Research Institute (Fig. 1; MRI, lat 36°04′N, long 140°07′E, 25 m a.s.l.) in Tsukuba, Ibaraki Prefecture, Japan. In this paper, we report the temporal variations in atmospheric CO_2 observed 200 m above the ground at the meteorological tower during the period from February 1992 through February 2000 and compare them with those of monitoring stations at the same latitudes. We elucidate year-to-year changes in the seasonal variation of atmospheric CO_2 observed from the meteorological tower, and investigate their relationship to the climate variables.

2. Method

2.1. Measurements of atmospheric CO_2

In this section, we briefly describe the CO_2 analyzing system that has been in use since April 1996 (Fig. 2). Systems used prior to April 1996 are given in Inoue and Matsueda (1996). In February 1992, we mounted an air intake on the tower at a height of 200 m above the ground; in April 1996, the same was done at 25 m. Air samples at 1.5 m above the ground and 30 m from the experimental field building are also drawn. The sampling lines were copper tubes (inner-diameter 8 mm, outer-diameter 10 mm at 200 m and 1.5 m above the ground; inner-diameter 4.35 mm, outer-diameter 6.35 mm at 25 m above the ground) that were coated on the outside with polyvinyl chloride. There was a total of 500 m of copper tube between the air intake at 200 m above the ground and the building. Air samples from the 3 heights were continuously pumped at a rate of 5 to 10 l min^{-1}, with most of the air being vented off. Aliquots of the air samples (0.45 l min^{-1}) were passed through 2 electric dehumidifiers, Nafion tubing (Perma Pure Inc.), and a column of magnesium perchlorate. These samples were then introduced into a non-dispersive infra-red gas analyzer (NDIR analyzer, Beckman model 865 or 880), which was placed in a plastic box (62 × 83 × 35 cm) to keep the temperature in the analyzer cell constant.

The NDIR analyzer was calibrated every 3 h by successively introducing 4 calibrated working gases (330, 360, 390, and 420 ppm CO_2 in dry air) into the NDIR analyzer cell for 6 min each. Measurements of atmospheric CO_2 were made every 6 min from the intakes at 25, 200, and 1.5 m and continued in this order until the next calibration. Three minutes after the change of gas flow, the output voltages of the NDIR analyzer were integrated at 1 Hz using a data logger (Nihon Denki Sanei, 7V-14) coupled to a PC (HP Vectra SF12 or VL5/166). Based on the replicate measurements of a sample gas in the cylinder, the precision of analysis ($\pm 1\sigma$) was estimated to be better than 0.1 ppm (Inoue and Matsueda, 1996). The output voltage of the NDIR analyzer was also recorded on an analogue recorder chart.

In this study, we discuss the temporal variations of atmospheric CO_2 based on hourly means calculated from the original CO_2 record. The % of the data compiled from 1 February 1992 to 29 February 2000 was 90% of the total (85% in 1992, 92% in 1993, 95% in 1994, 95% in 1995, 93% in 1996, 83% in 1997, 83% in 1998, 93% in 1999, and 96% in 2000).

2.2. Observation sites

The MRI is located on the Kanto Plain (Fig. 1), about 50 km northeast of Tokyo, 19 km south of Mt. Tsukuba (876 m a.s.l.), and 9 km west of Lake Kasumigaura (168 km^2). The city of Tsukuba (86.50 km^2) has a population of 163 000. Climatological data of surface temperature, precipitation, and flux of global solar radiation at the Tateno observatory (lat 36°03′N, long 140°08′E) in Tsukuba are listed in Table 1 (JMA, 2000). From January to August, the average surface

Fig. 1. Locations of the observation site for measurements of atmospheric CO_2 from the meteorological tower at the MRI in Tsukuba and stations monitoring atmospheric CO_2 in Japan and South Korea (upper panel), and the actual vegetation map in the central Japan (lower panel, http://www.biodic.go.jp/vg_map/vg_html/en/html/vg_map_frm_e.html).

A

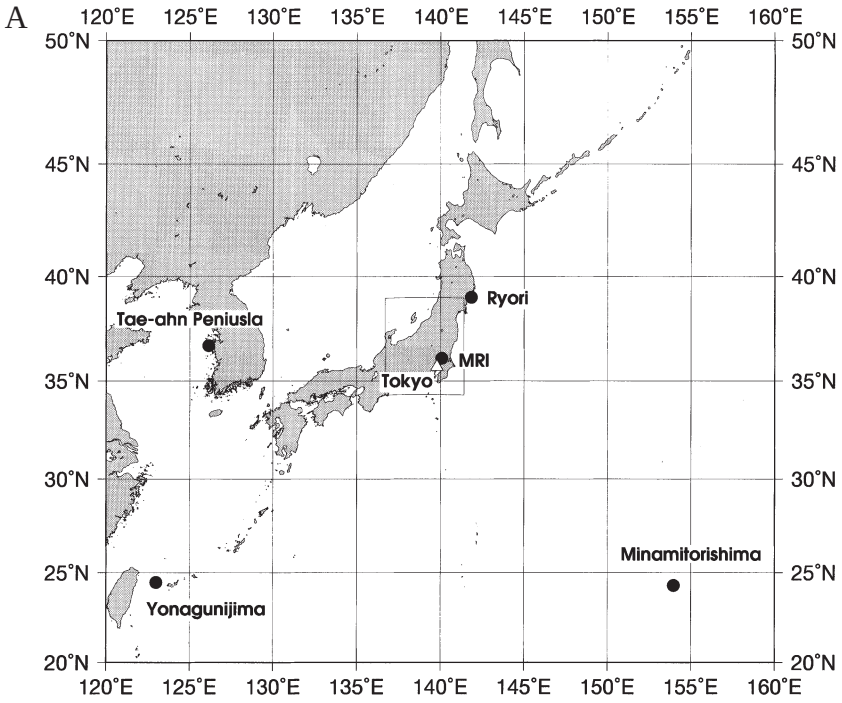
120°E
125°E
130°E
135°E
140°E
145°E
150°E
155°E
160°E
50°N
45°N
40°N
35°N
30°N
25°N
20°N
Tae-ahn Peniusla
Ryori
MRI
Tokyo
Minamitorishima
Yonagunijima

B

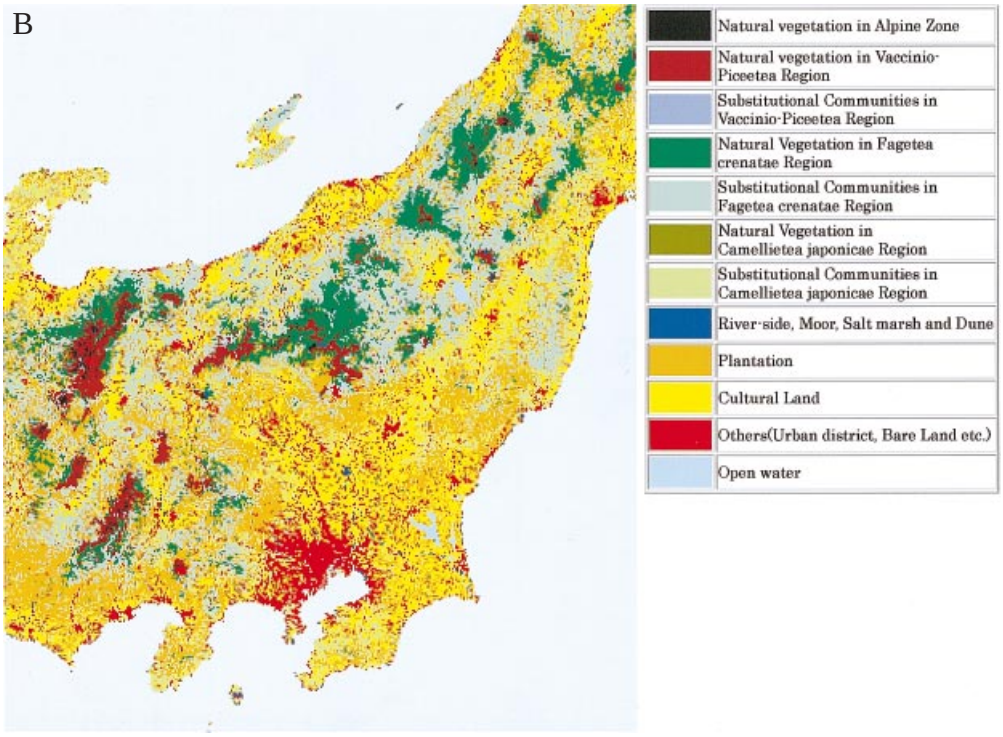
Natural vegetation in Alpine Zone
Natural vegetation in Vaccinio-Piceetea Region
Substitutional Communities in Vaccinio-Piceetea Region
Natural Vegetation in Fagetea crenatae Region
Substitutional Communities in Fagetea crenatae Region
Natural Vegetation in Camellietea japonicae Region
Substitutional Communities in Camellietea japonicae Region
River-side, Moor, Salt marsh and Dune
Plantation
Cultural Land
Others(Urban district, Bare Land etc.)
Open water

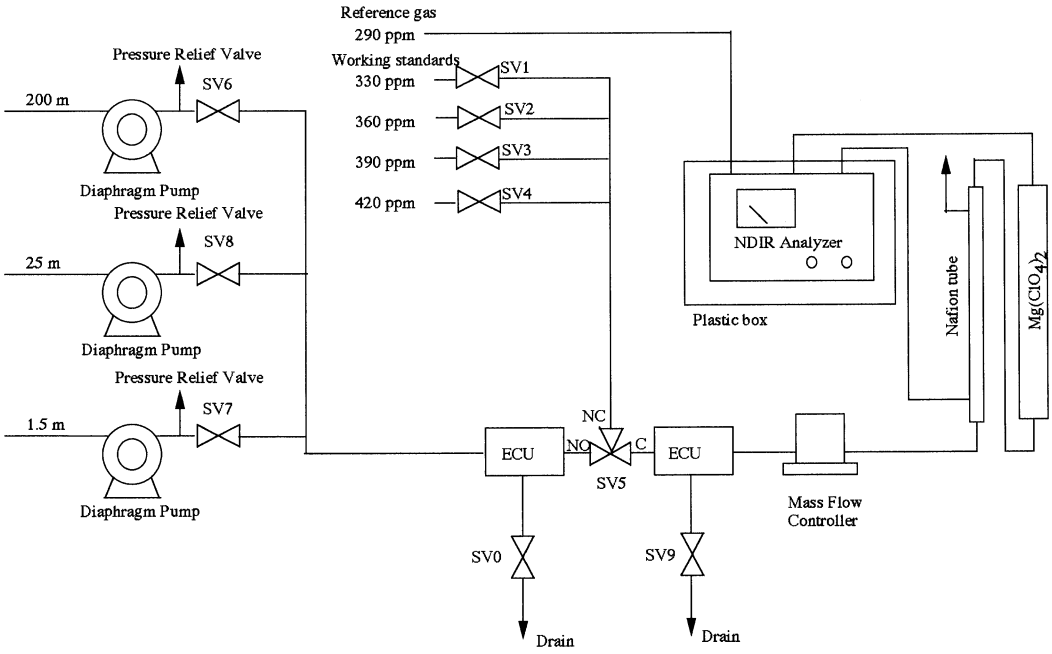

Fig. 2. Schematic diagram of the system used for measurements of atmospheric CO_2 since April 1996. SV refers to the solenoid valves, and ECU indicates the electric dehumidifiers, which can decrease the dew point to as low as 2 °C at a rate of 0.5 l min^{-1}.

Table 1. *Climatological data at the Tateno observatory (JMA, 2000)*

	Jan	Feb	Mar	Apr	May	Jun	Jul	Aug	Sep	Oct	Nov	Dec
T (°C)	1.9	2.9	6.1	12.0	16.6	19.9	23.5	25.2	21.3	15.2	9.6	4.1
P (mm)	35.5	54.7	82.7	101.5	121.2	159.7	121.7	120.3	153.3	138.3	74.7	38.7
R (MJ/m^2)	9.6	12.6	13.1	15.8	17.6	15.1	15.7	16.6	12.7	10.4	8.9	8.4

Averages of surface temperature and precipitation for the period from 1961 to 1990 and flux of global solar radiation for the period from 1990 to 1999.

temperature increases by 23 °C, and, from April to October, the mean monthly precipitation amount exceeds 100 mm. There is vegetation, forestation, cultural land, and urban area in and around the city. Vegetated areas consisting of deciduous and/or coniferous trees are located in and around the MRI grounds (0.32 km^2). The surface of the field where the meteorological tower stands is covered by thin organic clay soil, mostly overgrown with grasses. In January, the prevailing wind at 200 m is N to NW, and, in July, it is ENE or E followed by S (Report of Observation at the Meteorological Tower, 1994). The climatology and surface wind direction in Ibaraki Prefecture (MMO, 1959) exhibited similar trends to those observed at the meteorological tower.

Atmospheric CO_2 data from other monitoring stations Ryori (RYO, lat 39°02′ N, long 141°50′ E, 230 m a.s.l.), Minamitorishima (MNM, lat 24°18′ N, long 153°58′ E, 8 m a.s.l.), Yonagunijima (YON, lat 24°28′ N, long 123°01′ N, 30 m a.s.l.), Midway (MID, lat 28°13′ N, long 177°22′ W, 4 m a.s.l.), Bermuda East (BME, lat 32°22′ N, long 64°39′ W, 30 m a.s.l.), Bermuda West (BMW, lat 32°16′ N, long 65°33′ W, 30 m a.s.l.), Tae-ahn Peninsula (TAP, lat 36°44′ N, long 126°08′ E, 20 m a.s.l.) and airborne sampling using a commercial airliner (Matsueda and Inoue, 1996; JAL, lat

25–30°N, long 140–142°E, 10–13 km a.s.l.) were used for comparison. Throughout this paper the three-letter codes given above are used when referring to the monitoring stations. The first 3 ground sites are operated by the Japan Meteorological Agency (WMO WDCGG, 2000), and the remaining 4 ground sites are part of the National Oceanic and Atmospheric Administration/Climate Monitoring and Diagnostics Laboratory (NOAA/CMDL) flask-sampling network (Conway et al., 1994; Tans et al., 1998).

2.2. Standard gases

We classify our standard gases into three categories: primary, secondary, and working. Since 1987, we have been using primary standard gases (Nippon Sanso Co., Ltd.) that were gravimetrically prepared following the procedures reported by Tanaka et al. (1987). Working standard gases in aluminum cylinders (48 dm^3) were calibrated against the secondary standards before and after use. Equation (1) (Inoue and Matsueda, 1996) relates the CO_2 mixing ratios of our standards (expressed as ppm, $x\mathrm{CO}_2^{\mathrm{MRI87}}$) and the WMO 1985 mole-fraction scale ($x\mathrm{CO}_2^{\mathrm{WMO}}$):

$$x\mathrm{CO}_2^{\mathrm{WMO}} = 5.451 + 0.9741 x\mathrm{CO}_2^{\mathrm{MRI87}} + 2.7966 \times 10^{-5} (x\mathrm{CO}_2^{\mathrm{MRI87}})^2. \quad (1)$$

Eq. (1) is tentative and may undergo considerable changes in the future. In this paper, we report CO_2 mixing ratios based on the WMO 1985 mole-fraction scale as calculated by eq. (1).

Atmospheric CO_2 data presented here have been sent to the World Meteorological Organization World Data Center for Greenhouse Gases (WMO WDCGG, Tokyo), Japan and will be available in the near future.

2.3. Data selection

One of the objectives of measuring atmospheric CO_2 at 200 m is to determine CO_2 values representative of air on a regional-to-synoptic scale. Based on vertical profiles of temperature that indicated relatively strong vertical mixing during the daytime (Report of Observation at the Meteorological Tower, 1997) and the diurnal variation of atmospheric CO_2 mixing ratios at 1.5 m and 200 m (Subsection 3.1), we first calculated average CO_2 values between 1300 and 1600 JST. Because the raw data at 200 m occasionally exhibited extremely high values, which are probably due to the effects of local sources, we have omitted values higher than 390 ppm (2% of the total) in the present work. Consequently, 88% of the data over the period from 1 February 1992 through 29 February 2000 was retained. A time series analysis of this CO_2 record was made by a method similar to that used by Thoning et al. (1989):

$$x\mathrm{CO}_2(t) = A_0 + A_1 t + A_2 t^2 + A_3 t^3 + A_4 t^4 + \sum_{i=1}^{3} [B_i \cos(\omega, t) + C_i \sin(\omega, t)], \quad (2)$$

where t denotes the time in years since 1 January 1992 and A_i, B_i, and C_i are constants. CO_2 mixing ratio data differing from the curve by more than $2\times$ the residual standard deviation ($1\sigma = 6.1$ ppm) were removed. The amount of data retained was 85% of the total. The remaining data were again fitted to eq. (2) by the method of least squares. We then calculated the differences between retained CO_2 data and values obtained by eq. (2) over the period from 1 February 1992 to 29 February 2000. If the data of the difference between the retained CO_2 data and the value obtained by eq. (2) were missing, gaps were filled by linear interpolation between contiguous data. A low-pass filter with a cutoff point at 100 days (Hanning filter, Igor 1.26) was designed to examine the temporal variations on a time scale of a few months and applied to the continuous residual data. Before the application of the low-pass filter, the continuous residual data were extended by 365 days at each end of the series by repeating the first and last years of data (Thoning et al., 1989). After applying the low-pass filter, the residual standard deviation was calculated to be 4.7 ppm. In order to analyze the long-term CO_2 trend, a low-pass filter with a cutoff point at 667 days (Hanning filter, Igor 1.26) was designed and applied to the data. The sum of the filtered data and the first 5 terms on the right-hand side of eq. (2) are treated as the long-term trend.

As a criterion for baseline stations, Thoning et al. (1989) retained any 2 consecutive hourly averages where the hour-to-hour difference was smaller than 0.25 ppm. For a comparison with baseline stations, we selected CO_2 data showing hour-to-hour differences of less than 0.25 ppm. The retained data

amounted to 71% of the total, and, from the calculated results, the mean difference between daily mean CO_2 data for the time 1300–1600 JST and CO_2 data selected by hour-to-hour variability smaller than 0.25 ppm was 2 ppm with a standard deviation of 1 ppm ($n = 2951$).

3. Results and discussion

3.1. Diurnal variation

Fig. 3 shows atmospheric CO_2 mixing ratios at 1.5, 25, and 200 m above the ground from the meteorological tower in Tsukuba over 3 days in January and August 1999. In the period of 8–10 January 1999, the atmospheric CO_2 mixing ratio at 200 m was fairly constant and lower than those of 1.5 and 25 m. In the period of 5–7 August 1999, the atmospheric CO_2 mixing ratio at 200 m showed a maximum in the morning and a minimum in the late afternoon. During the daytime, the atmospheric CO_2 mixing ratio varied less as compared with that of the nighttime and morning and was slightly larger than that of 1.5 m between 930 and 1530 JST.

The monthly mean of diurnal variation of atmospheric CO_2 at 200 m above the ground, calculated from unselected data, showed quite a different pattern from that found at 1.5 m (Fig. 4). The influence of variability on synoptic scales was removed by subtracting the daily mean value of the CO_2 mixing ratio at 200 m from the observed values. As reported earlier (Inoue and Matsueda, 1996), CO_2 mixing ratios in the air at 1.5 m show significant diurnal variation throughout the year: the average amplitude during diurnal variation was 26 ppm in January and 49 ppm in August. In January, the diurnal variation of atmospheric CO_2 at 200 m above the ground was not as clear as in August (Fig. 4), when the largest diurnal variation occurred at 200 m (13 ppm). In August, the maximum of atmospheric CO_2 at 200 m above the ground occurred a few hours after dawn (0800

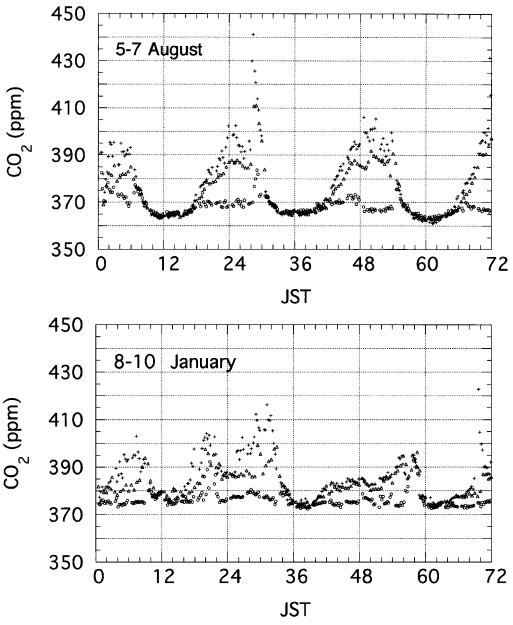

Fig. 3. Atmospheric CO_2 mixing ratio at 1.5, 25, and 200 m above the ground from the MRI meteorological tower in Tsukuba over three-day periods (8–10 January 1999 and 5–7 August 1999). The plus symbol, the open triangle, and the open circle mean the atmospheric CO_2 mixing ratio at 1.5 m, 25 m, and 200 m, respectively.

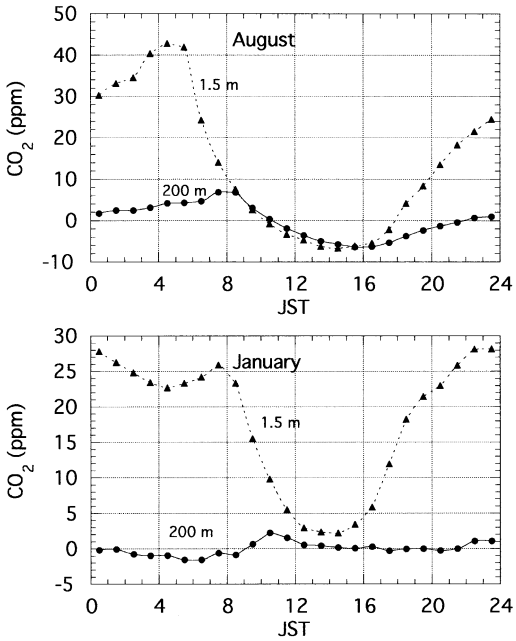

Fig. 4. Diurnal variations in atmospheric CO_2 at 1.5 (solid triangle) and 200 m (solid circle) above the ground from the meteorological tower in Tsukuba. The daily mean value at 200 m above the ground was subtracted from observed values for each day. Data are composite for the month of January between 1993 and 2000, and August between 1992 and 1999.

JST), and the minimum was observed at 1600 JST. At 1.5 m, the maximum of atmospheric CO_2 occurred just before dawn, and the minimum was recorded at 1400–1500 JST (Fig. 4). The maximum of atmospheric CO_2 at 200 m was caused by the upward mixing of CO_2 stored in the nocturnal stable layer with the onset of convection (Bakwin et al., 1995). Data from a Doppler Sodar installed at the MRI typically indicated that the convective boundary layer developed at the rate of a few cm s^{-1} during the summer season (Fig. 2-1, in Takeuchi, 1997). In summer, the minimum of atmospheric CO_2 occurred during the daytime due to the photosynthesis of land plants and strong vertical mixing of air. During the plant growth season, CO_2 mixing ratios at 200 m above the ground were as high as 1 ppm compared with those at 1.5 m, and the local time showing a higher CO_2 mixing ratio at 200 m varied from year to year (Fig. 5). In winter, the level of photosynthesis/respiration of land plants was much lower, and the diurnal variation of atmospheric CO_2 at 1.5 m was mainly caused by anthropogenic CO_2 sources and the strong temperature inversion that developed during the night (Inoue and Matsueda, 1996). From mid-night to 0800 JST, the CO_2 mixing ratio of atmospheric CO_2 at 200 m was fairly low and constant as a result of the temperature inversion formed between 50 and 100 m during the winter time (Report of Observation at the Meteorological Tower, 1997).

3.2. *Comparison of CO_2 data with those of baseline/regional stations*

Atmospheric CO_2 record at 200 m above the ground in Tsukuba (Fig. 6) showed seasonal variations similar to those observed at baseline stations in northern mid-latitudes; this is caused by the CO_2 exchange between the air and the land biosphere (Conway et al., 1994; GLOBALVIEW-CO_2, 1997). CO_2 mixing ratios reached their maximum in April and their minimum in late August or early September. Monthly and annual means of CO_2 mixing ratios at 200 m (Table 2) were compared with those of stations located at latitudes between 24 and 40°N (Fig. 7). Daily mean values of atmospheric CO_2 at 200 m in Tsukuba between 1300 and 1600 JST usually showed the highest values among these stations. The annual mean CO_2 mixing ratios at stations in remote areas (MNM, MID, BME, and BMW) and the upper troposphere (JAL) were as high as 1–4 ppm compared to that of the South Pole (SPO, Conway et al., 1994; Tans et al., 1998) and 4–9 ppm at stations close to/in the eastern edge of the Eurasian Continent (YON, TAP, and RYO, MRI). If net CO_2 uptake or CO_2 emission from the land biosphere does not occur during the annual cycle, the increase of the CO_2 mixing ratio is caused by the CO_2 emission due to fossil fuel combustion. The population surrounding the observational site (Fukushima Pref., Ibaraki

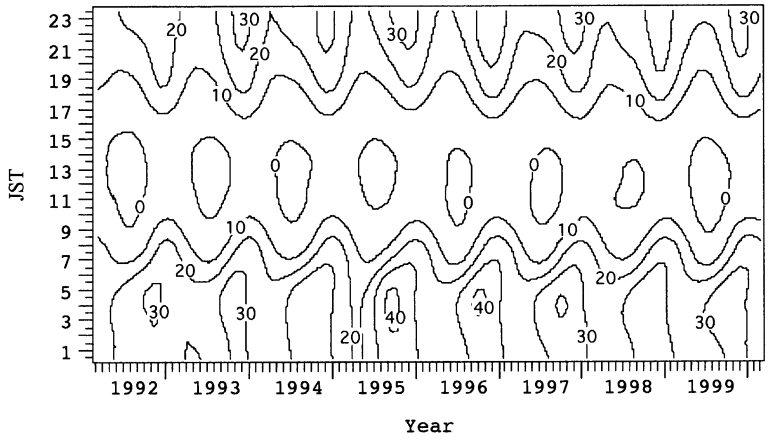

Fig. 5. Differences between CO_2 mixing ratios at 1.5 m and 200 m (xCO_2 at 1.5 m–xCO_2 at 200 m) during the period from February 1992 through February 2000. To draw contours, a matrix was made by interpolating and smoothing the original data.

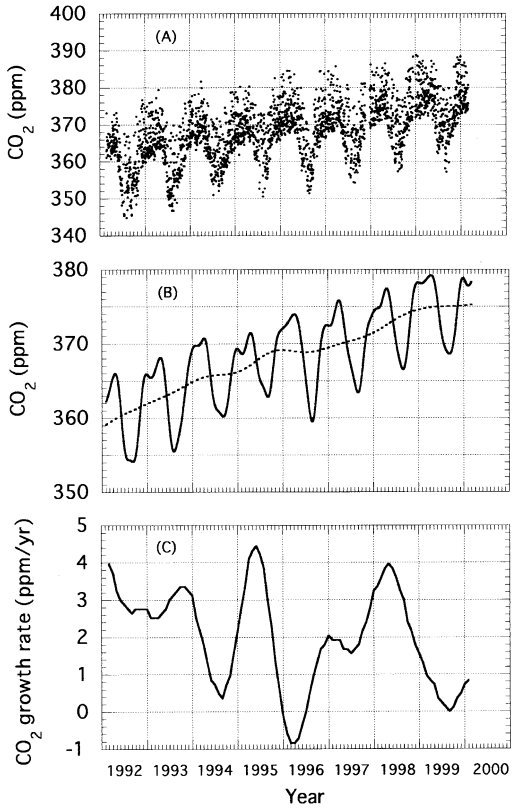

Fig. 6. Temporal variations in the daily means of selected atmospheric CO_2 data at 200 m from February 1992 through February 2000. The top panel (A) shows the selected data used for curve fitting. The solid curve in (B) is the result of a low-pass filter with a cutoff point at 100 days, the dashed curve is the result of a filter with a cutoff point at 667 days, and the dash-dotted curve includes extrapolated data (see text). The low panel (C) shows the growth rate of atmospheric CO_2.

Prefecture, Chiba Pref., Gunma Pref., Tochigi Prefecture, Saitama Pref., and Tokyo Metropolis; total area: 44×10^3 km^2) was 32.9×10^6. Assuming a per-capita CO_2 emissions (2.54 metric tons C per year; Marland et al., 1999) and an average planetary boundary layer depth over Tsukuba (1000 m, Gamo, 1984), CO_2 emissions due to human activity were estimated to increase CO_2 levels by approximately 10 ppm. This figure was fairly consistent with the tower data, which show the atmospheric CO_2 level as high as 4–6 ppm when compared with those of stations in remote areas (MNM, MID, BME, and BMW). Bakwin et al. (1998) have reported that measurements of CO_2 mixing ratios from very tall towers (496 and 396 m) give an approximate measure of the mixing ratios in the afternoon convective boundary layer (within a few tenths of a ppm). We have not yet examined to what degree the present data are representative. However, they are probably within a few ppm because there is only a small difference between the present data and data selected by the criteria used to obtain the representative value of the well-mixed air at baseline stations (Subsection 2.3).

Annual CO_2 emission from Japan reported by Marland et al. (1999) correlated well with the annual energy consumption of fossil fuel expressed as the crude petroleum equivalence reported by the Ministry of International Trade and Industry (Inoue and Matsueda, 1996). If we assume a linear relation between energy consumption and CO_2 emissions, it is possible to estimate seasonal variations in CO_2 emissions on the basis of monthly energy consumption data. From spring to summer, monthly CO_2 emission was estimated to increase by 4% (Inoue and Matsueda, 1996). If atmospheric CO_2 at the meteorological tower increases by 4–6 ppm due to CO_2 emissions from fossil fuel combustion, the contribution of seasonal change in CO_2 emissions to the observed CO_2 is $\sim$0.2 ppm, which is small compared with the year-to-year changes in the seasonal variation of atmospheric CO_2.

Over the period from 1993 to 1999, the atmospheric CO_2 observed from the meteorological tower increased from 363.0 to 374.6 ppm (Table 2). The growth rate of atmospheric CO_2 between February 1992 and January 2000 showed a large interannual variability that ranged from -0.8 to 4.6 ppm/yr^{-1} at a mean rate of 2.0 ppm yr^{-1} (Fig. 6-C). Superimposed on the growth rate of atmospheric CO_2 in remote areas is the effect of changes in sources/sinks up to a synoptic scale and/or air masses of different origins.

3.3. *Interannual variability of seasonal variation in atmospheric CO_2*

Interannual variations in the peak-to-trough amplitude of the seasonal variation of atmospheric CO_2 have been examined to elucidate the CO_2 exchange between the air and the land biosphere, especially related to the CO_2 fertilization effect

Table 2. *Monthly means of CO_2 mixing ratios in the air (ppm) 200 m above the ground on the meteorological tower in Tsukuba*

Year	Month	Mean	SD ($1-\sigma$)	Median	n	Smoothed data
1992	January	—	—	—	—	—
	February	364.8	4.0	363.2	6	362.6
	March	364.2	2.0	364.8	17	364.5
	April	365.1	2.7	364.8	30	365.6
	May	364.5	3.7	364.1	29	363.3
	June	357.0	4.9	355.5	28	357.8
	July	355.6	7.5	357.9	14	354.5
	August	355.5	5.4	354.8	29	354.1
	September	352.8	4.1	353.4	28	354.2
	October	357.0	5.1	356.3	30	357.3
	November	362.2	5.7	364.2	20	362.6
	December	365.6	5.5	363.5	29	365.4
Annual mean						
1993	January	364.9	4.1	363.8	30	365.3
	February	366.0	4.6	364.0	28	365.5
	March	366.6	3.7	366.1	27	366.8
	April	367.7	3.9	366.6	29	367.7
	May	366.6	3.9	366.1	29	365.9
	June	361.7	4.7	362.1	27	360.7
	July	355.0	6.0	352.5	28	356.1
	August	354.9	6.1	354.7	30	355.8
	September	356.4	3.9	355.6	19	357.8
	October	361.1	4.6	360.7	29	361.1
	November	365.2	5.3	365.4	19	365.1
	December	367.4	3.9	366.5	22	368.1
Annual mean		362.8		362.0		363.0
1994	January	370.0	3.7	370.4	26	369.4
	February	367.7	3.7	366.7	20	369.5
	March	369.4	2.9	369.7	28	370.0
	April	371.4	4.2	371.6	30	370.0
	May	366.4	4.0	366.2	31	366.8
	June	361.7	4.0	361.7	26	362.7
	July	360.5	5.2	360.4	29	360.9
	August	361.1	5.6	362.7	26	360.3
	September	360.0	4.3	359.4	27	360.2
	October	362.4	4.8	360.6	29	362.4
	November	366.0	4.1	365.6	26	366.2
	December	368.6	4.7	367.3	28	368.7
Annual mean		365.4		365.2		365.6

(Keeling et al., 1996). Detrended seasonal variations (Fig. 8) were calculated by subtracting values of the long-term trend from the smoothed values in Fig. 6-B. Table 3 lists the maximum above the long-term trend and the minimum below the trend. Considering the days where CO_2 reaches a maximum or a minimum, which are not very well determined due to the flatness of the

Table 2 *(contd)*

Year	Month	Mean	SD ($1-\sigma$)	Median	n	Smoothed data
1995	January	369.2	4.3	367.7	31	368.7
	February	368.2	3.8	367.1	25	368.5
	March	369.7	3.4	370.1	30	369.9
	April	371.0	3.9	370.6	29	371.0
	May	369.6	3.4	369.2	22	369.2
	June	364.4	3.8	362.7	29	366.0
	July	365.5	5.6	365.8	19	364.3
	August	363.7	6.5	365.5	23	363.1
	September	361.2	4.8	360.4	30	363.2
	October	367.6	4.2	366.3	26	366.8
	November	371.1	4.0	369.8	29	370.3
	December	370.4	3.5	369.9	29	371.5
Annual mean		367.6		367.1		367.7
1996	January	372.7	5.1	370.8	30	372.0
	February	372.5	3.6	372.1	27	372.7
	March	373.9	4.9	374.2	30	373.4
	April	372.5	3.8	371.5	29	373.4
	May	371.9	3.7	371.9	25	371.3
	June	367.2	5.9	368.4	27	367.2
	July	364.0	4.5	363.6	22	362.8
	August	358.0	5.1	357.9	23	359.7
	September	359.4	4.6	358.0	27	361.4
	October	368.3	4.4	368.4	28	366.9
	November	370.8	5.5	369.7	29	371.0
	December	372.1	4.3	371.8	27	372.2
Annual mean		368.6		368.2		368.7
1997	January	371.3	4.0	370.9	28	372.2
	February	373.2	4.4	372.7	27	373.3
	March	374.2	5.0	373.8	18	375.1
	April	374.1	3.3	373.3	25	374.5
	May	370.2	3.4	369.9	27	371.1
	June	367.6	5.9	366.2	26	368.0
	July	365.3	6.9	365.1	22	365.6
	August	364.2	5.8	365.8	21	363.6
	September	364.0	4.6	363.9	27	364.2
	October	369.4	5.8	368.4	28	368.2
	November	371.9	4.5	372.0	18	371.8
	December	374.0	4.1	374.6	7	373.4
Annual mean		370.0		369.7		370.1

smoothed detrended seasonal variation, Conway et al. (1988) examined the phase of the seasonal variation in the CO_2 mixing ratios by determining the days when the decreasing and increasing mixing ratios cross the line of the long-term trend. These days were used as indicators of the phasing of CO_2 drawdown (DD) and buildup (BU), respectively. The present record indicates that both DD and BU occur on nearly the same days each year (± 8 days), but the peak-to-trough ampli-

Table 2 *(contd)*

Year	Month	Mean	SD ($1-\sigma$)	Median	n	Smoothed data
1998	January	375.5	4.8	374.2	27	374.
	February	374.8	4.1	374.5	23	374.5
	March	374.5	3.2	374.0	28	375.7
	April	377.9	3.6	377.8	25	377.0
	May	375.4	5.1	374.4	31	375.4
	June	370.9	5.0	370.3	20	371.8
	July	367.7	6.3	367.2	23	368.6
	August	368.0	6.3	368.0	29	366.6
	September	365.3	4.6	364.8	25	367.3
	October	372.4	4.6	371.3	25	371.4
	November	375.6	5.2	374.3	25	375.8
	December	376.8	5.0	376.0	14	377.7
Annual mean		372.9		372.2		373
1999	January	377.5	5.2	376.2	30	377.8
	February	378.0	4.8	377.2	26	378.0
	March	378.5	3.8	378.0	31	378.5
	April	377.5	2.9	377.6	23	378.8
	May	378.5	4.1	378.1	31	377.3
	June	372.9	6.1	373.2	26	373.4
	July	370.3	4.9	370.1	28	370.1
	August	368.8	5.0	369.5	30	368.6
	September	368.3	5.2	368.7	29	368.6
	October	369.8	3.0	369.3	21	371.0
	November	374.9	4.7	373.4	28	375.3
	December	379.2	5.1	378.5	31	378.2
Annual mean		374.5		374.1		374.6
2000	January	377.6	3.9	376.7	30	377.9
	February	376.8	3.4	375.7	27	377.6

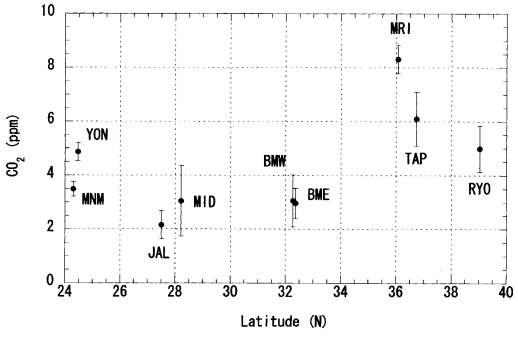

Fig. 7. The annual mean of the CO_2 mixing ratio at stations located between 24 and 40°N relative to the annual mean of the South Pole. The error bars represent the maximum and minimum difference at each station from that of SPO over the period from 1992 to 1998.

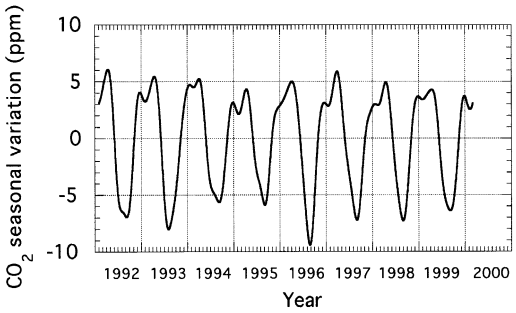

Fig. 8. Detrended seasonal variation in atmospheric CO_2 at 200 m from the meteorological tower in Tsukuba, central Japan, during the period from February 1992 to February 2000.

Table 3. *Seasonal variations in atmospheric CO_2 200 m above the ground from the meteorological tower in Tsukuba*

Year	Peak-to-trough amplitude	Maximum	Minimum	DD	BU
1992	13.1	6.1	−7.0	3 June	7 November
1993	13.5	5.5	−8.0	5 June	7 November
1994	10.9	5.3	−5.6	25 May	12 November
1995	10.3	4.4	−5.9	31 May	29 October
1996	14.4	5.0	−9.4	7 June	27 October
1997	13.1	5.9	−7.2	26 May	3 November
1998	12.2	4.9	−7.3	7 June	1 November
1999	10.7	4.3	−6.4	6 June	11 November

DD means the day when decreasing CO_2 mixing ratio cross the line of long-term trend and BU the day when increasing CO_2 mixing ratio cross the line of long-term trend (Fig. 6).

tude of the seasonal variation varied considerably from year to year (Table 3). This suggests that steep changes in CO_2 mixing ratio during and after the plant growth season play an important role in determining the maximum/minimum values of atmospheric CO_2 mixing ratios. In order to examine year-to-year changes in seasonal variation, we selected the change in the CO_2 mixing ratio over fixed periods that varied rapidly and monotonously, namely, the change in CO_2 mixing ratio of the detrended seasonal variation (ΔCO_2) from 1 May to 31 July and that from 1 September to 31 October. The change of CO_2 mixing ratios for 1 May to 31 July was as large as 84% of the peak-to-trough amplitude of the seasonal variation and 51% for 1 September to 31 October.

Year-to-year differences in the seasonal variation in atmospheric CO_2 could be caused by changes in biological activity or by air masses of different origins (Bakwin et al. 1998). First, we examined the relationship between ΔCO_2 and climate variables. Photosynthesis/respiration are influenced by environmental conditions including temperature, precipitation, solar radiation, soil texture, and atmospheric CO_2 mixing ratio (see, e.g., VEMAP MEMBERS, 1995). Within natural variations of the first three climate variables (temperature, precipitation, and solar radiation), the factors controlling ΔCO_2 were examined by assuming the multiple linear function eq. (3):

$$\Delta CO_2 = a \times T_{av} + b \times P_{av} + c \times R_{av} + d, \qquad (3)$$

where a, b, c, and d are parameters that were determined by the least squares method. In eq. (3), we used the averages of temperature (T_{av}), precipitation amount (P_{av}), and flux of global solar radiation (R_{av}) observed at the Tateno observatory (JMA, 2000). The climate data at the Tateno observatory can be thought of as representative because climate anomalies usually occur on regional-to-synoptic scales.

During the period from 1 May to 31 July, ΔCO_2 shows a good correlation with the T_{av} (Table 4; Fig. 9). Climate variables in eq. (3) are likely to be correlated with air masses of different origins. However, discussing the biological activity and air masses of different origins on the basis of a regional carbon cycle model is beyond the scope of the present work. The atmospheric CO_2 level from the meteorological tower for the period from 1 May to 31 July is almost always the highest among those CO_2 monitoring stations located north and south of the MRI (Fig. 10). If air masses of different origins play an important role in determining year-to-year changes in ΔCO_2, the CO_2 mixing ratio decreases whether an air mass originated from the south with high temperature or from the north with low temperature sits over central Japan for some time from 1 May to 31 July. A good T_{av}-ΔCO_2 relationship suggests that the effect of biological activity over central Japan on changes in ΔCO_2 could be large as compared with that of air masses of different origins.

If biological activity over central Japan affected ΔCO_2 during the period from 1 May to 31 July, we can hypothesize the temperature dependence of the photosynthesis/respiration rates. The increase (decrease of the absolute value) of ΔCO_2 with the increase of T_{av} means the decrease in the net CO_2 uptake with T_{av}, which can be explained

Table 4. *Correlation coefficient matrix of multiple linear regression analysis for changes in CO_2 mixing ratio of detrended seasonal variation*

	1 February–31 March			1 May–31 July			1 September–31 October		
	P_{av}	R_{av}	ΔCO_2	P_{av}	R_{av}	ΔCO_2	P_{av}	R_{av}	ΔCO_2
T_{av}	−0.114	−0.312	0.577	−0.243	0.607	0.780	0.123	−0.456	−0.552
P_{av}		−0.301	−0.186		−0.707	0.013		−0.559	0.249
R_{av}			−0.337			0.236			0.219

(ΔCO_2) against average surface temperature (T_{av}), precipitation amount (P_{av}), and flux of global solar radiation (R_{av}).

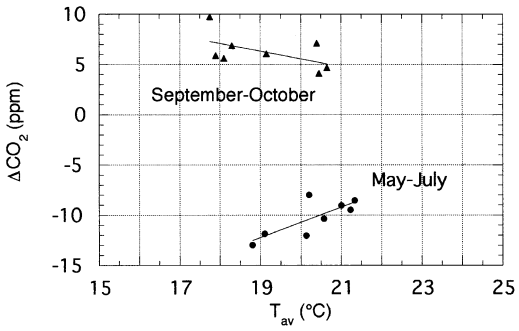

Fig. 9. Relationship between average surface temperature (T_{av}) of daily mean values in Tsukuba and changes in CO_2 mixing ratios (ΔCO_2) of detrended seasonal variations over the periods from 1 February to 31 March (solid square), 1 May to 31 July (solid circle) and 1 September to 31 October (solid triangle). Detrended seasonal variations of atmospheric CO_2 were calculated by subtracting the values of the long-term trend from the smoothed values (see text).

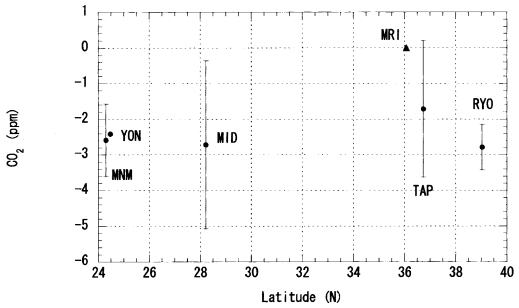

Fig. 10. Mean value of the atmospheric CO_2 mixing ratio at stations in and around Japan over the period from May to July relative to that of the meteorological tower at 200 m above the ground in Tsukuba. The error bars represent the maximum and minimum difference at each station from that of the meteorological tower at 200 m over the period from 1992 to 1998.

by the larger temperature dependence of respiration rate as compared with that of photosynthesis rate. IPCC (1990) reports that gross photosynthesis of many mid-latitude plants occurs at an optimum rate in the range of 20 to 35 °C. The rate of plant respiration tends to be slow below 20 °C; however, at higher temperatures, the respiration rate accelerates rapidly up to a temperature at which it equals the rate of gross photosynthesis and there can be no net assimilation of carbon. In the present work, we do not take into account year-to-year changes in the depth of planetary boundary layer to discuss changes in ΔCO_2, because no clear relationship between the depth of planetary boundary layer and surface air temperature has been reported in Tsukuba (Gamo, 1984).

In September, CO_2 uptake by photosynthesis in a temperate deciduous forest in Japan remained at a level nearly equal to that during the plant growth season, and in October decreased considerably (Yamamoto et al., 1999). The atmospheric CO_2 mixing ratio showed a clear positive upward gradient up to 4 km over Japan (Nakazawa et al., 1993). In September and October, the CO_2 mixing ratio at 200 m above the ground in Tsukuba was always the highest (0.1–7.6 ppm) among CO_2 monitoring stations in Fig. 10 located north and south of the MRI. Therefore, the increase of the CO_2 mixing ratio at 200 m above the ground in Tsukuba from 1 September to 31 October was mainly caused by the vertical mixing with the upper air and the decrease of CO_2 uptake by photosynthesis in October. For the period from 1 September to 31 October, ΔCO_2 correlated mostly with T_{av} among climate variables, but correlation was low as compared with that during the period from 1 May to 31 July (Table 4).

To examine the T_{av}-ΔCO_2 relationship in differ-

ent season, we selected the period from 1 February to 31 March. The amospheric CO_2 mixing ratio of the detrended seasonal variation increased rather gradually at a low surface temperature over the period from 1 Fabruary to 31 March. Over this period, ΔCO_2 also correlated well to T_{av} and increased with T_{av}, which was opposite to the temperature dependence of ΔCO_2 from 1 September to 31 October (Table 4).

The present results show the apparent temperature dependence of ΔCO_2 on regional-to-synoptic scales, which should provide a constraint to biogeochemical carbon cycle models. These T_{av}-ΔCO_2 relationships could change depending on the species of land plants and the climate. It is clear that monitoring CO_2 in the lower troposphere over areas of land plants is necessary to determine the "integrated" CO_2 exchange between the air and the land biosphere, and its future change associated with climate change.

4. Acknowledgments

The authors wish to express their gratitude to Mr. Matsuura of the Meteorological Satellite and Observation System Department, MRI for preparing the meteorological data from the meteorological tower and to the staff of the Geochemical Research Department, MRI for their helpful discussions. The constructive criticism of two anonymous reviewers helped to improve the manuscript.

REFERENCES

Bakwin, P. S., Zhao, C., Ussler III, W., Tans, P. P. and Quesnell, E. 1995. Measurements of carbon dioxide on a very tall tower. *Tellus* **47B**, 535–549.

Bakwin, P. S., Tans, P. P., Hurst, D. F. and Zhao, C. 1998. Measurements of carbon dioxide on very tall towers: results of the NOAA/CMDL program. *Tellus* **50B**, 401–415.

Conway, T. J., Tans, P., Waterman, L. S., Thoning, K. W., Masarie, K. A. and Gammon, R. H. 1988. Atmospheric carbon dioxide measurements in the remote global troposphere, 1981–1984. *Tellus* **40B**, 81–115.

Conway, T. J., Tans, P. P., Waterman, L. S., Thoning, K. W., Kitzis, D. R., Masarie, K. A. and Zhang, N. 1994. Evidence for interannual variability of the carbon cycle from the National Oceanic and Atmospheric Administration/Climate Monitoring and Diagnostics Laboratory Global Air Sampling Network. *J. Geophys. Res.* **99**, 22,831–22,855.

Gamo, M. 1984. Seasonal change of the heat balance in the mixed layer. *Kogai* **19**, 11–24 (in Japanese).

GLOBALVIEW-CO_2. 1997. *Cooperative Atmospheric Data Integration Project-Carbon Dioxide. 1997.* CD-ROM, NOAA/CMDL, Boulder, CO. FTP, ftp.cmdl.noaa.gov, Path: ccg/CO2/GLOBALVIEW.

Haszpra, L. 1995. Carbon dioxide concentration measurements at a rural site in Hungary. *Tellus* **47B**, 17–22.

Inoue and Matsueda. 1996. Variations in atmospheric CO_2 at the Meteorological Research Institute, Tsukuba, Japan. *J. Atmos. Chem.* **23**, 137–161.

IPCC. 1990. Intergovernmental Panel on Climate Change (IPCC). *Climate Change: The IPCC Scientific Assessment*, edited by J. T. Houghton, G. J. Jerkins and J. J. Ephraums. Cambridge University Press. New York.

IPCC. 1995. Intergovernmental Panel on Climate Change (IPCC). *Climate Change 1995. The Science of Climate Change*, edited by J. T. Houghton, L. G. M. Meira Filho, B. A. Callander, N. Harris, A. Kattenberg and K. Maskell. Cambridge University Press. New York.

JMA. 2000. *Annual Report of the Japan Meteorological Agency*. Japan Meteorological Agency, Tokyo.

Keeling, C. D., Bacastow, R. B., Carter, A. F., Piper, S. C., Whorf, T. P., Heimann, M., Mook, W. G. and Roeloffzen, H. 1989. A three-dimensional model of atmospheric CO_2 transport based on observed winds: (1). Analysis of observational data. In: *Aspects of climate variability in the Pacific and western America*, edited by D. M. Peterson. pp. 165–236. AGU Geophysical Monograph. Washington D.C.

Keeling, C. D., Chin, J. F. S. and Whorf, T. P. 1996. Increased activity of northern vegetation inferred from atmospheric CO_2 measurements. *Nature* **358**, 723–727.

Kuc, T. 1991. Concentration and carbon isotopic composition of atmospheric CO_2 in southern Poland. *Tellus* **43B**, 373–378.

Levin, I. 1987. Atmospheric CO_2 in continental Europe, an alternative approach to clean air CO_2 data. *Tellus* **39B**, 21–28.

Levin, I., Graul, R. and Trivett, N. B. A. 1995. Long-term observations of atmospheric CO_2 and carbon isotopes at continental sites in Germany. *Tellus* **47B**, 23–34.

Marland, G., Boden, T., Brenkert, A., Andres, B. and Johnston, C. 1999. National CO_2 Emissions from Fossil-Fuel Burning, Cement Manufacture, and Gas Flaring: 1751–1996. In: *Trends online, A compendium of date on global change*. http://cdiac.esd.ornl.gov/ftp/ndp030/nation96.ems

Matsueda, H. and Inoue, H. Y. 1996. Measurements of atmospheric CO_2 and CH_4 using a commercial airliner from 1993 to 1994. *Atmos. Environ.* **30**, 1647–1655.

MMO. 1959. Ibaraki-ken no Kikou (*The climate of Ibaraki Prefecture*), Mito Meteorological Observatory (in Japanese). pp. 15–16. Japan Meteorological Association. Tokyo.

Nakazawa, T., Morimoto, S., Aoki, S. and Tanaka, M. 1993. Time and space variations of the carbon isotopic ratio of tropospheric carbon dioxide over Japan. *Tellus* **45B**, 258–274.

Report of Observation at the Meteorological Observation Tower. 1997. No. 6 (1994–1996), pp. 1–48. Meteorological Research Institute. Tsukuba, Japan.

Schmidt, M., Graul, R., Sartorius, H. and Levin, I. 1996. Carbon dioxide and methane in continental Europe: a climatology, and ^{222}Radon-based emission estimates. *Tellus* **48B**, 457–473.

Takeuchi, K. 1997. Wind in the planetary boundary layer. In: *Meteorology of the wind* (Lectures on Meteorology 4, in Japanese), pp. 7–48. University of Tokyo Press, Tokyo.

Tanaka, M., Nakazawa, T. and Aoki, S. 1987. Time and space variations of tropospheric carbon dioxide over Japan. *Tellus* **39B**, 3–12.

Tans, P. P. 1991. An observational strategy for assessing the role of terrestrial ecosystems in the global carbon cycle: scaling down to regional levels. In: *Scaling processes between leaf and landscape levels*, edited by J. Ehleringer and C. Field. Academic Press, San Diego.

Tans, P. P., Bakwin, P. S., Bruhwiler, L., Conway, T. J., Dlugokencky E. J., Guenther, D. W., Hurst, D. F., Kitzis, D. R., Lang, P. M., Masarie, K. A., Miller, J. B., Novelli, P. C., Prostoko-Bell, C., Thoning, K. W., Vaughn, B. H., White, J. W. C., Yakir, D. and Zhao, C. 1998. Carbon Cycle, ch. 2, in *Climate monitoring and diagnostics laboratory*, Summary report no. 24, 1996–1997, edited by D. J. Hofmann, J. T. Peterson and R. M. Rosson, pp. 30–51. NOAA Environ. Res. Labs., Boulder, CO., USA.

Thoning, K. W., Tans, P. P. and Komhyr, W. D. 1989. Atmospheric carbon dioxide at Mauna Loa Observatory. 2. Analysis of the NOAA GMCC data 1974–1985. *J. Geophys. Res.* **94**, 8549–8565.

VEMAP Members, 1995. VEMAP: A comparison of biogeography and biogeochemistry models in the context of global climate change. *Global Biogeochem. Cycles* **9**, 407–437.

WMO WDCGG. 2000. World Meteorological Organization. Global Atmosphere Watch. World Data Center for Greenhouse Gases. WMO WDCGG DATA REPORT. WDCGG No. 21. Japan Meteorological Agency, Tokyo, Japan.

Yamamoto, S., Murayama, S., Saigusa, N. and Kondo, H. 1999. Seasonal and interannual variation of CO_2 flux between a temperate forest and the atmosphere in Japan. *Tellus* **51B**, 402–413.